

## Knotting and supercoiling in circular DNA: A model incorporating the effect of added salt

M. C. Tesi,<sup>1</sup> E. J. Janse van Rensburg,<sup>2</sup> E. Orlandini,<sup>1</sup> D. W. Sumners,<sup>3</sup> and S. G. Whittington<sup>1</sup>

<sup>1</sup>*Department of Chemistry, University of Toronto, Toronto, Ontario, Canada M5S 1A1*

<sup>2</sup>*Department of Mathematics, York University, North York, Ontario, Canada M3J 1P3*

<sup>3</sup>*Department of Mathematics, Florida State University, Tallahassee, Florida 32306-3027*

(Received 5 August 1993)

We consider a model of a circular polyelectrolyte, such as DNA, in which the molecule is represented by a polygon in the three-dimensional simple cubic lattice. A short-range attractive force between non-bonded monomers is included (to account for solvent quality) together with a screened Coulomb potential (to account for the effect of added salt). We compute the probability that the ring is knotted as a function of the number of monomers in the ring, and of the ionic strength of the solution. The results show the same general behavior as recent experimental results by Shaw and Wang [Science **260**, 533 (1993)] and by Rybenkov, Cozzarelli, and Vologodskii [Proc. Natl. Acad. Sci. U.S.A. **90**, 5307 (1993)] on the knot probability in circular DNA as a function of added salt. In addition, we compute the writhe of the polygon and show that this also increases as the ionic strength increases. The writhe computations model the conformational behavior of nicked circular duplex DNA molecules in salt solution.

PACS number(s): 87.10.+e

### I. INTRODUCTION

Many biologically interesting polymers, such as DNA and RNA, are highly charged polyelectrolytes and their conformational properties will be sensitive to the charge density along the polymer chain and to the ionic strength of the solution in which they are dissolved. In particular, the entanglement complexity of the polymer depends sensitively on the ionic strength, and this has been modeled by Klenin *et al.* [1] by varying the effective diameter of the polymer chain. In the case of DNA the incidence of topological entanglements such as knotting and catenation is critical to the functioning of the cell [2] and, for this reason, there exist enzymes to control the geometry and topology of DNA, especially during replication and recombination. *In vitro* and *in vivo* topological enzymology experiments utilize supercoiling, knotting, and catenation of circular DNA to study the mechanism and synaptic complex structure of enzymes such as topoisomerase and recombinase [3–5]. The conformation of DNA *in vivo* depends on the cellular environment, which is essentially an aqueous solution containing dissolved electrolytes. It is thus imperative to understand the dependence of the geometry and topology of DNA on the electrolyte concentration in cellular fluids.

Partly as a result of this, there has been a considerable amount of work on the detection of knots in circular DNA [6,7] and, more recently, in determining the knotting probability as a function of parameters such as the length of the DNA molecule and the ionic strength of the solution [8,9]. In particular, Shaw and Wang [8] recently determined the frequency of occurrence of knotted conformations upon cyclization of linear duplex DNA molecules with 5.6 and 8.6 kilo-base-pairs, in aqueous solutions containing varying amounts of NaCl and MgCl<sub>2</sub>. The linear DNA substrates were designed to have single stranded “sticky” ends similar to phage  $\lambda$ . These ends

are cohesive, and cyclization of the DNA traps DNA topoisomers in the form of knots. Similar results were obtained by Rybenkov, Cozzarelli, and Vologodskii [9] for cyclization of linear DNA with 10 kilo-base-pairs. Since DNA is a polyelectrolyte in which each monomer carries a charge of the same sign, the Coulombic interaction between these charges will be repulsive and will yield an effective diameter greater than the geometric diameter of DNA. This Coulombic repulsion will be shielded by the ions in solution, and so the effective diameter of the polymer should decrease as the ionic strength of the solution is increased. This will result in more compact linear objects, which are more likely to be knotted upon cyclization. This expectation is born out in the experiments of Shaw and Wang [8] and Rybenkov, Cozzarelli, and Vologodskii [9] which show that the probability of obtaining nontrivial topoisomers depends strongly on the ionic strength of the solution; the knot probability increases significantly with increasing ionic strength.

There have been two complementary approaches in theoretical work on knotting in models of ring polymers. One approach has been to prove rigorous results about the asymptotic behavior, in the limit when the rings become infinitely large [10–14]. The most important conclusion of these works is that the knot probability converges exponentially rapidly to unity as the size of the ring polymer goes to infinity, thus giving an affirmative answer to the conjecture of Frisch and Wasserman [15] and Delbruck [16].

The other main approach which has been used to study the knot probability relies on Monte Carlo methods [1,17–21]; in fact, although Monte Carlo techniques are limited to quite short rings, they can give quantitative results for particular models. In Sec. III we report the results of a Monte Carlo study of the knot probability of a ring polymer in solutions with various ionic strengths.

The mechanism of enzyme-mediated knotting and

catenation of covalently closed circular duplex DNA in solution is thought to comprise two steps. The molecule supercoils due to the backbone strand linking deficit, solvent quality and ion concentration, and enzymes such as topoisomerase then allow strand passage via transient enzyme-bridged single- and double-strand breaks in the DNA chain. In order to study the dependence of supercoiling on the ionic strength of the solvent, it is interesting to examine geometrical complexity measures such as the writhe of the polygon. Writhe has proved to be a useful quantity in modeling the degree of supercoiling in DNA [22,23]. In Sec. IV we report some Monte Carlo results on the dependence of the writhe of a ring polyelectrolyte on the ionic strength of the solution.

## II. DESCRIPTION OF THE MODEL

Lattice models of polymers offer considerable advantages both from theoretical and computational points of view. In the cubic lattice,  $Z^3$ , ring polymers are conveniently modeled by polygons, i.e., by a sequence of distinct vertices such that successive pairs are nearest neighbors and are connected by edges, and the last vertex is a nearest neighbor of the first and connected to it by an edge. The vertices in the polygon represent the monomers (or sets of monomers) in the ring polymer, and the edges represent the chemical bonds connecting the monomers (Fig. 1). There are efficient Monte Carlo algorithms for simulating polygons in the cubic lattice [24] which can be used to compute thermodynamic equilibrium properties for the model considered in this paper, and the algorithm can be efficiently implemented through the use of integer data structures such as hash tables.

Previous Monte Carlo work on knot probabilities has focused on models with only a short-range repulsive force between monomers in the ring, or with a short-range repulsion and an additional attractive force to mimic the effect of varying the quality of the solvent [20]. In this study we modify these models to include a screened Coulomb potential between the monomers, where the screening can be varied to account for the effect of added

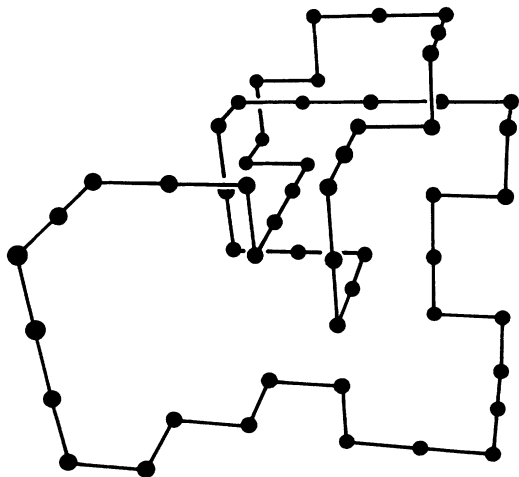


FIG. 1. A trefoil on the cubic lattice with  $n = 54$ .

electrolyte. This kind of interaction can be approximated by a Yukawa-type potential which represents the effective ion-ion potential in a Debye-Hückel model for ions in a continuum dielectric solvent [25]. The total potential energy of a polygon in this model is

$$U = \sum_{i < j} [u(r_{ij}) + A e^{-\kappa r_{ij}} / r_{ij}],$$

where  $r_{ij}$  is the distance between the  $i$ th and  $j$ th vertices of the polygon, measured in lattice units, and the sum is over all nonbonded pairs of vertices. The first term,  $u(r)$ , is equal to  $kTv$  if  $r=1$  and zero otherwise, where  $v$  is a negative constant. We chose for  $v$  the value  $-0.26$  since it is known that, for the simple cubic lattice, it corresponds to a poor solvent regime [26], in which the knot probability is higher and easier to study. The second term in the potential energy is the Yukawa term which accounts for the screened Coulomb interaction between the charges on the monomers of the polyelectrolyte.  $\kappa^{-1}$  is the Debye length measured in lattice units and its value reflects the ionic strength of the solution. The parameter  $A$  is connected to the charge density along the polymer chain, and to a length scale in the polymer, such as the persistence length. We do not expect the main features of the behavior to depend very sensitively on the value of  $A$  and, to check this, we have carried out calculations for a range of values of  $A$  stretching over two decades.

We have investigated the properties of this model using a Metropolis Monte Carlo approach based on pivots [24]. The conformation space is explored by making proposed changes in the conformation of the polygon by choosing a pair of vertices at random and modifying the shorter part of the polygon between these two vertices, to obtain a new polygon. The new polygon is accepted with a probability chosen to make the limiting distribution the Boltzmann distribution with  $U$  as the associated energy.

## III. ESTIMATES OF THE KNOT PROBABILITY

Determining whether or not a polygon is knotted is a nontrivial matter. However, provided that the knot is not too complex, it can be detected by computing the Alexander polynomial  $\Delta(t)$  of the polygon [17], evaluated at  $t = -1$ . If  $\Delta(-1) \neq 1$  the polygon is knotted. [This is not a perfect detector of knotting since it is possible for  $\Delta(-1) = 1$  for a knotted polygon. However, this occurs with extremely low probability for polygon lengths that we are considering in this paper.] The Monte Carlo simulation was run for  $2.5 \times 10^6$  iterations while the knot type of the polygons was determined every 50 iterations, giving a sample size of 50 000 for each data point. Averages and variances over the sample size were computed by estimating autocorrelation times over suitably chosen windows. All error bars in the figures are one standard deviation.

In Fig. 2 we show the dependence of the knot probability on  $\kappa$  for polygons of three sizes,  $n = 200, 300,$  and  $400$ , with  $A/kT = 0.01$ . It is clear from this figure that the knot probability increases as  $n$  increases, at fixed  $\kappa$ , and increases as  $\kappa$  increases at fixed  $n$ . It seems that the knot probability levels off to a relatively small value as  $\kappa$  be-

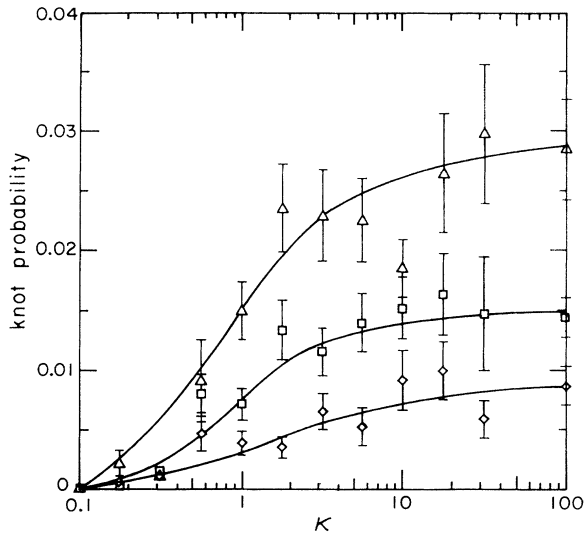


FIG. 2. The knot probability as a function of  $\kappa$ , for polygons with  $n=200$  ( $\diamond$ ),  $300$  ( $\square$ ), and  $400$  ( $\triangle$ ).  $\kappa$  is in units of reciprocal-lattice spacings.

comes very large. When  $\kappa$  is sufficiently large, the Coulombic repulsion is effectively negligible so that this behavior is consistent with previous findings that the knot probability is quite small at those values of  $n$ , even in a poor solvent [20]. For a 1-1 electrolyte,  $\kappa$  is proportional to the square root of the concentration of the ions, so we can compare Fig. 2 with the experimental results of Shaw and Wang [8] for a solution containing NaCl. The behavior is very similar, and our results confirm the general shapes of the curves drawn through the experimental points in that paper. To investigate the influence of the charge density on the knot probability we repeated the calculations of knot probability for  $A/kT=0.1$  and  $1$ , with  $n=300$ . The results are shown in Fig. 3. The same general behavior occurs at each value of  $A$ , although the sigmoidal portion of the curve moves to higher values of

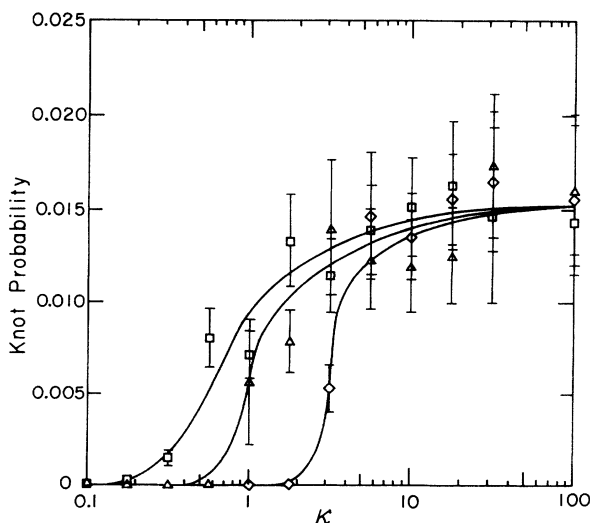


FIG. 3. The knot probability as a function of  $\kappa$  for  $n=300$  with  $A/kT=0.01$  ( $\square$ ),  $A/kT=0.1$  ( $\triangle$ ), and  $A/kT=1$  ( $\diamond$ ).

$\kappa$  as  $A$  increases. That is, as the charge density along the polymer increases, a smaller value of the Debye length is required for the knot probability to increase markedly.

We also studied the probability of formation of various knot types as a function of  $\kappa$ . In Table I we report their distribution for polygons of length  $n=300$  and  $400$ , and  $A/kT=0.01$ . It is clear that as  $\kappa$  increases not only does the number of knots increase but so does their complexity.

We expect that increasing the ionic strength will lead to a decrease in the overall dimensions of the molecule and we have confirmed this by calculating the mean-square radius of gyration as a function of  $n$  and  $\kappa$ . The results are shown in Fig. 4. The mean-square radius of gyration drops rapidly as  $\kappa$  increases, and then settles to a plateau. This change in the dimensions is much more marked for larger  $n$ . An alternative way to characterize this change in the compactness is to focus on the number of pairs of vertices which are nearest neighbors on the lattice. We show  $\langle C_n \rangle$ , the mean number of first-neighbor vertex pairs (or contact number), as a function of  $\kappa$ , for different values of  $n$ , in Fig. 5. There is a marked increase in this measure of compactness as  $\kappa$  increases, as expected since the contact number is known to be positively correlated with the increasing knot probability in polygons [20]. We conclude that increasing the ionic strength of the solution is equivalent to reducing the quality of the solvent and hence increasing the knot probability. We also know that more complicated knots have smaller dimensions [27], which is consistent with the observation that these knots have higher electrophoretic mobility than less complicated ones [28].

TABLE I. Table of knot distribution (%) as a function of  $\kappa$  for two polygons of length  $n=300$  and  $400$ , respectively.

$\kappa$	$\Delta(-1)$	1	3	5	$\geq 7$
$n=300$					
0.1	99.96	0.04	0.00	0.00	0.00
0.32	99.83	0.17	0.00	0.00	0.00
0.56	99.25	0.74	0.00	0.00	0.00
1	99.36	0.79	0.05	0.00	0.00
1.78	98.59	1.34	0.03	0.04	0.00
3.16	98.27	1.60	0.13	0.00	0.00
10	98.23	1.77	0.04	0.00	0.00
17.78	98.59	1.40	0.01	0.00	0.00
31.62	98.53	1.45	0.02	0.01	0.00
100	98.30	1.23	0.47	0.00	0.00
$n=400$					
0.1	99.99	0.01	0.00	0.00	0.00
0.32	99.81	0.19	0.00	0.00	0.00
0.56	99.22	0.67	0.01	0.00	0.00
1	98.77	1.11	0.12	0.00	0.00
1.78	97.77	2.07	0.04	0.12	0.00
3.16	98.06	1.74	0.13	0.07	0.00
10	97.98	1.91	0.10	0.01	0.01
17.78	97.27	2.25	0.27	0.21	0.00
31.62	96.33	3.37	0.28	0.02	0.00
100	96.80	2.98	0.19	0.03	0.00

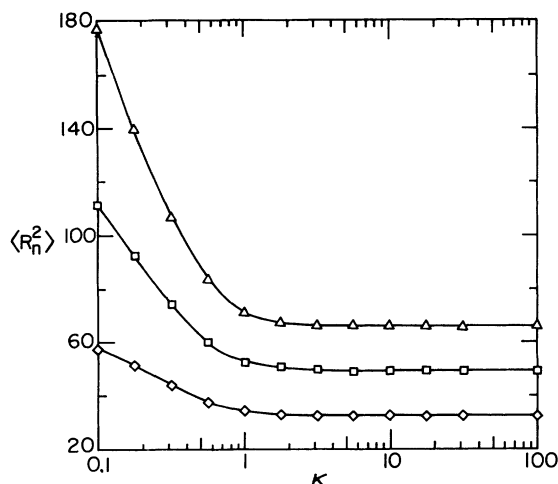


FIG. 4. The dependence of the mean-square radius of gyration  $\langle R_n^2 \rangle$  on  $\kappa$  for polygons with  $A/kT=0.01$ ,  $n=200$  ( $\diamond$ ), 300 ( $\square$ ), and 400 ( $\triangle$ ). The error bars are smaller than the size of the symbols.  $\kappa$  is in units of reciprocal-lattice spacings, and the mean-square radius of gyration is in units of lattice spacing squared.

#### IV. ESTIMATES OF THE WRITHE

The writhe of a polygon is a geometrical property, not a topological one. To define writhe consider any simple closed curve in  $R^3$ , and project it onto  $R^2$  in some direction  $\hat{x}$ . In general, the projection will have crossings and, for almost all projection directions, these crossings will be transverse, so that we can associate a sign  $+1$  or  $-1$  with each crossing, as in Fig. 6. For this projection we form the sum of these signed crossing numbers,  $S(\hat{x})$ , and then average over all projection directions  $\hat{x}$ . This average quantity is the writhe  $W$  of the curve [29]. Writhe is a geometrical quantity (since it is not invariant under ambient isotopy) and is a real number which mea-

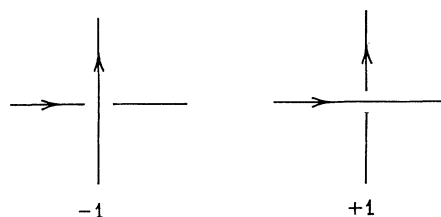


FIG. 6. Positive and negative crossings are determined by a right-hand rule.

sures the extent to which the polygon is supercoiled.

In principle, one needs to average the sum of the signed crossing numbers over all (regular) projections but there is a useful theorem [30] which considerably simplifies the calculation for polygons on lattices. For self-avoiding polygons in  $Z^3$ , the computation of the writhe can be reduced to the average of linking numbers of the given curve with four selected pushoffs [30].

In Fig. 7 we show the dependence of the expectation of the absolute value of the writhe on  $\kappa$  for  $n=400$ , for  $A/kT=0.01$  and 0.1. The writhe increases with  $\kappa$  for small values of  $\kappa$  and then levels off to a plateau. This is somewhat different from the behavior of the knot probability and, in particular, the plateau is reached for smaller values of  $\kappa$ . At small values of  $\kappa$  the writhe depends noticeably on the value of  $A$  but both curves approach the same plateau value as  $\kappa$  increases. Increasing the charge density decreases the writhe at small  $\kappa$  but, as the Debye length decreases, and the screening therefore increases, the writhe becomes almost independent of the charge density.

#### V. SUMMARY AND DISCUSSION

The model used in this paper is a very simple one. Its essential features are the nonrigid nature of the lattice polygon (which models the entropy of the ring), the short-

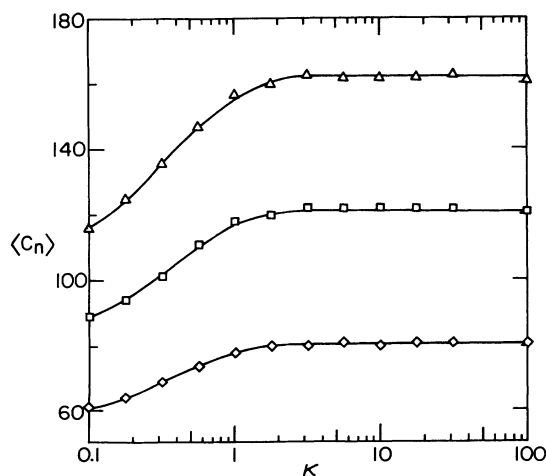


FIG. 5. The dependence of the mean number of contacts  $\langle C_n \rangle$  on  $\kappa$  for polygons with  $A/kT=0.01$ ,  $n=200$  ( $\diamond$ ), 300 ( $\square$ ), and 400 ( $\triangle$ ). The error bars are smaller than the size of the symbols.

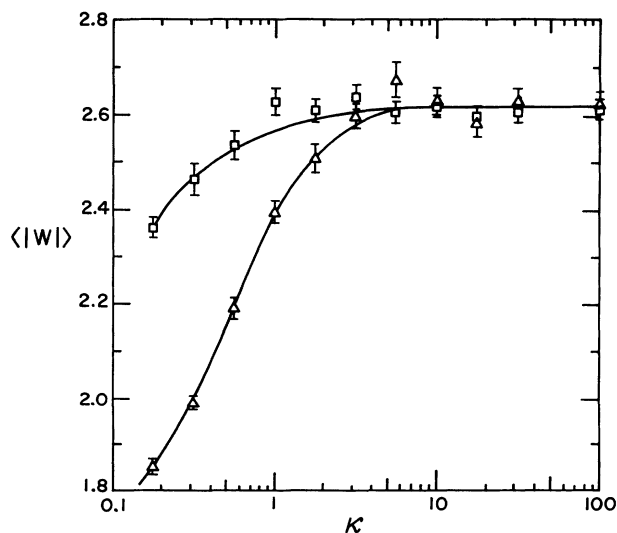


FIG. 7. The dependence of the average of the absolute value of the writhe on  $\kappa$  for  $n=400$ ,  $A/kT=0.01$  ( $\square$ ), and  $A/kT=0.1$  ( $\triangle$ ).

range attraction between monomers (which models the solvent quality), and the screened Coulomb potential (which models the effect of the added electrolyte). Although it contains no detailed chemical or physical properties of DNA and neglects details of the local structure, nevertheless it gives good qualitative and semiquantitative agreement with the experimental results on closed circular DNA. We deduce that the variation of the knot probability with ionic strength, observed experimentally, is primarily determined by a combination of the entropy of the ring, the solvent quality, and the screening of the

Coulombic potential due the added electrolyte. In addition we have presented computations of the writhe as a function of ionic strength, and have shown that this quantity is also sensitive to the concentration of ions in the electrolyte solution.

#### ACKNOWLEDGMENTS

We are pleased to acknowledge financial support from the NSERC of Canada and the NSF of the United States of America.

- 
- [1] K. V. Klenin, A. V. Vologodskii, V. V. Anshelovich, A. M. Dykhne, and M. D. Frank-Kamenetskii, *J. Biomol. Str. Dyn.* **5**, 1173 (1988).
- [2] K. Shishido, N. Komiyama, and S. Ikawa, *J. Mol. Biol.* **195**, 215 (1987).
- [3] S. A. Wasserman and N. R. Cozzarelli, *Science* **232**, 951 (1986).
- [4] D. W. Sumners, *Math. Intelligencer* **12**, 71 (1990).
- [5] C. Ernst and D. W. Sumners, *Math. Proc. Camb. Philos. Soc.* **108**, 489 (1990).
- [6] F. B. Dean and N. R. Cozzarelli, *J. Biol. Chem.* **260**, 4984 (1985).
- [7] S. A. Wasserman and N. R. Cozzarelli, *J. Biol. Chem.* **266**, 20567 (1991).
- [8] S. Y. Shaw and J. C. Wang, *Science* **260**, 533 (1993).
- [9] V. V. Rybenkov, N. R. Cozzarelli, and A. V. Vologodskii, *Proc. Natl. Acad. Sci. U.S.A.* **90**, 5307 (1993).
- [10] H. L. Frisch and D. Klempner, *Adv. Macromol. Chem.* **2**, 149 (1970).
- [11] W. S. Kendall, *J. London Math. Soc.* **19**, 378 (1979).
- [12] D. W. Sumners and S. G. Whittington, *J. Phys. A* **21**, 1689 (1988).
- [13] N. Pippenger, *Discrete Appl. Math.* **25**, 273 (1989).
- [14] C. E. Soteros, D. W. Sumners, and S. G. Whittington, *Math. Proc. Camb. Philos. Soc.* **111**, 75 (1992).
- [15] H. L. Frisch and E. Wasserman, *J. Am. Chem. Soc.* **83**, 3789 (1961).
- [16] M. Delbruck, in *Mathematical Problems in the Biological Sciences*, Proceedings of the Symposium on Applied Mathematics (American Mathematical Society, Providence, RI, 1962), Vol. 14, p. 55.
- [17] A. V. Vologodskii, A. V. Lukashin, M. D. Frank-Kamenetskii, and V. V. Anshelevich, *Zh. Eksp. Teor. Fiz.* **66**, 2153 (1974) [*Sov. Phys. JETP* **39**, 1059 (1974)].
- [18] M. D. Frank-Kamenetskii, A. V. Lukashin, and A. V. Vologodskii, *Nature* **258**, 398 (1975).
- [19] J. P. J. Michels and F. W. Wiegel, *Proc. R. Soc. A* **403**, 269 (1986).
- [20] E. J. Janse van Rensburg and S. G. Whittington, *J. Phys. A* **23**, 3573 (1990).
- [21] K. Koniaris and M. Muthukumar, *J. Chem. Phys.* **95**, 2873 (1991).
- [22] W. R. Bauer, F. H. C. Crick, and J. H. White, *Sci. Am.* **243**, 118 (1980).
- [23] J. H. White and W. R. Bauer, *J. Mol. Biol.* **189**, 329 (1986).
- [24] N. Madras, A. Orlicsky, and L. A. Shepp, *J. Stat. Phys.* **58**, 159 (1990).
- [25] S. Glasstone, *An Introduction to Electrochemistry* (Van Nostrand, Princeton, N.J., 1942).
- [26] E. J. Janse van Rensburg, D. W. Sumners, E. Wasserman, and S. G. Whittington, *J. Phys. A* **25**, 6557 (1992).
- [27] E. J. Janse van Rensburg and S. G. Whittington, *J. Phys. A* **24**, 3935 (1991).
- [28] H. A. Lim and E. J. Janse van Rensburg, SCRI Report No. FSU-SCRI-91-163 (1991) (unpublished).
- [29] F. B. Fuller, *Proc. Natl. Acad. Sci. U.S.A.* **68**, 815 (1971).
- [30] R. C. Lacher and D. W. Sumners, in *Computer Simulations of Polymers*, edited by R. J. Roe (Prentice-Hall, Englewood Cliffs, 1991), p. 365.